Structural Engineering and Mechanics, Vol. 29, No. 1 (2008) 91-111
DOI: http://dx.doi.org/10.12989/sem.2008.29.1.091

Computational modeling of coupled fluid-structure systems with applications

Y. Kerboua[†] and A.A. Lakis[‡]

Mechanical Engineering Department, École Polytechnique de Montréal, C.P. 6079, Succursale Centre-ville, Montréal, Quebec, H3C 3A7, Canada

M. Thomas[‡†]

Mechanical Engineering Department, École de Technologie Supérieure, 1100 Notre Dame Ouest Montréal, Quebec, H3C 1K3, Canada

L. Marcouiller[‡‡]

Institut de Recherche d'Hydro Quebec, 1800 Lionel-Boulet, Varennes, Quebec, J3X 1S1, Canada

(Received April 9, 2007, Accepted February 1, 2008)

Abstract. This paper outlines the development of a computational model in order to analyze the dynamic behaviour of coupled fluid-structure systems such as a) liquid containers, b) a set of parallel or radial plates. In this work a hybrid fluid-solid element is developed, capable of simulating both membrane and bending effects of the plate. The structural mass and stiffness matrices are determined using exact integration of governing equations which are derived using a combination of classical plate theory and a finite element approach. The Bernoulli equation and velocity potential function are used to describe the liquid pressure applied on the solid-fluid element. An impermeability condition assures a permanent contact at the fluid-structure interface. Applications of this model are presented for both parallel and radial plates as well as fluid-filled rectangular reservoir. The effect of physical parameters on the dynamic behaviour of a coupled fluid-structure system is investigated. The results obtained using the presented approach for dynamic characteristics such as natural frequency are in agreement to those calculated using other theories and experiments.

Keywords: plates and shells; added mass; vibration; fluid-solid element.

1. Introduction

Plates and shells constitute important components of complex structures for modern applications in fields such as construction engineering, aerospace and aircraft structures, nuclear power plant

† Ph.D., E-mail: youcef.kerboua@polymtl.ca
‡ Professor, Corresponding author, E-mail: aouni.lakis@meca.polymtl.ca
‡† Professor, E-mail: marc.thomas@etsmtl.ca
‡‡ Ph.D., E-mail: marcouiller.luc@ireq.ca

components and naval structures. Structural systems composed of parallel plates, rectangular reservoirs as well as turbine hubs can be considered as shell-type structures. Often these structures work in interaction with either a stationary or flowing fluid, which has a considerable influence on their dynamic responses. The first works in the fluid-structure interaction domain were developed in the nineteenth century by Rayleigh (1945) and Lamb (1945). These works constitute the fundamental theory of fluid-filled cylindrical and spherical shells. Later, Berry and Reissner (1958) studied the behaviour of a fluid-filled cylindrical shell under pressure. Vibration analysis of partially fluid-filled cylindrical shells was investigated by Lindholm *et al.* (1962). Lakis and Paidoussis (1971) developed a circumferential hybrid element based on classic shell theory for dynamic analysis of a partially fluid-filled cylindrical shell. The vibration responses of an orthotropic cylindrical shell filled with an incompressible fluid were calculated by Jain (1974). Amabili and Dalpiaz (1995) developed an analytical approach to model a horizontal cylindrical shell, partially or fully filled with fluid. Selmane and Lakis (1997) developed a longitudinal hybrid element for dynamic analysis of open and closed horizontal cylindrical shells which are either partially or fully filled with liquid.

Circular and rectangular plates in interaction with fluid were the subject of a large number of research works since the beginning of the twentieth century. The effects of boundary conditions, the free surface of the fluid and fluid level as well as the membrane effect have been studied using experiments and computational approaches in Lamb (1920), Lindholm *et al.* (1965), Fu and Price (1987), Kwak (1994, 1997), Amabili and Kwak (1999) and Kwak and Han (2000). A detailed bibliographic survey on plate dynamic behaviour in interaction with a stationary fluid is outlined in Kerboua *et al.* (2005).

Jeong *et al.* (1998) analytically studied the dynamic behaviour of two identical circular plates coupled with the movement of an ideal incompressible fluid using the Rayleigh method. Precise results were obtained for the case of in-phase modes whereas results for out-of-phase modes were unsatisfactory except for mode $m = 0$. In order to improve the out-of-phase lateral vibration frequencies, Jeong (2003) applied Fourier-Bessel's finite set and Rayleigh-Ritz's approach to re-analyze his former model and this time obtained very satisfactory results. Jeong *et al.* (2004) studied the case of two identical rectangular plates coupled with the movement of fluid. Kim and Lee (1997) analyzed the hydro-elastic behaviour of an open rectangular reservoir completely filled with water based on the MSC/NASTRAN DMAP's formulation. Only the first two frequencies for the in-phase and out-of-phase modes are analytically calculated. Bauer (1981) studied the hydro-elastic behaviour of a completely or partially fluid-filled rectangular reservoir. This container is composed of rigid lateral walls and an elastic plate that forms its base. Cheung and Zhou (2000) calculated the natural frequencies of a plate forming the base of an open rectangular reservoir completely filled with liquid. The fluid-free surface effect was not considered in this calculation. The case of a circular plate composing the base of a rigid cylindrical tank filled with fluid was studied by Cheung and Zhou (2002) by considering the fluid free surface effect. The velocity potential function was used to model the fluid media and the Galerkin approach was adopted to calculate the natural frequencies of the coupled system. Santanu and Sinhamahapatra (2005) studied the coupled slosh dynamics of fluid-filled containers. They calculated natural frequencies of sloshing and also studied the forced vibration responses of the fluid-structure system. A semi analytical method was developed by Ding and Weiqing (2007) to study the three dimensional vibration of flexible rectangular tanks partially filled with liquid. The vibrating modes of liquid-tank system are divided to various distinct categories each of these categories is separately investigated. The bulging and

sloshing mode were considered.

The objective of this work is to develop a computational model based on a fluid-plate element to study the dynamic responses of fluid-structure systems, i.e., a set of parallel or radial plates which could represent turbine blades that are in contact with an incompressible and non-viscous fluid. This new element also permits calculation of the high and low frequencies of the system with precision and can take into account any combination of boundary conditions without changing the displacement field. This hybrid element is applied to simulate a number of industrial structures such as a set of parallel or radial plates in vacuum or submerged in fluids.

2. Structural modeling

2.1 Mass and stiffness matrices of a plate in local co-ordinates

A typical finite element in its local coordinates is shown in Fig. 1. Each element is presented by four nodes (*i*, *j*, *k*, *l*) and five degrees of freedom at each node consisting of three displacements and two rotations. The in-plane displacement functions are represented by bilinear polynomials and the out-of-plane displacement functions are derived from the plate's equation of equilibrium (details are presented in references Kerboua *et al.* 2005). The in-plane displacement field is defined as

$$U(x,y,t) = C_1 + C_2\frac{x}{A} + C_3\frac{y}{B} + C_4\frac{xy}{AB} \tag{1a}$$

$$V(x,y,t) = C_5 + C_6\frac{x}{A} + C_7\frac{y}{B} + C_8\frac{xy}{AB} \tag{1b}$$

where U and V are the displacement components of the reference surface in X and Y directions, respectively. A and B are the plate dimensions in X and Y directions. The transversal displacement component of the reference surface is defined as

$$W(x,y,t) = \sum_{j=9}^{20} C_j e^{i\pi\left(\frac{x}{A}+\frac{y}{B}\right)} e^{i\omega t} \tag{2}$$

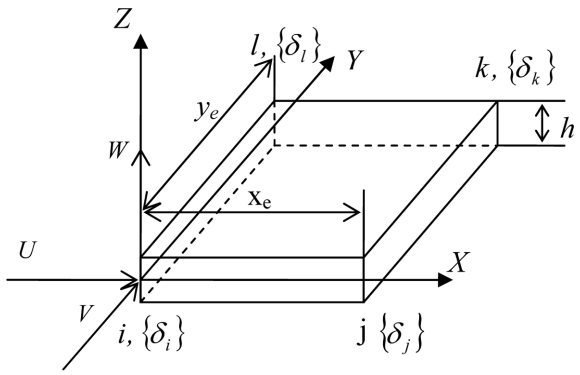

$$\{\delta_i\} = \{U_i, V_j, W_i, W_{i,x}, W_{i,y}\}^T$$

Fig. 1 Finite element geometry and nodal displacement vector in local co-ordinates *X*, *Y*, *Z*

where W is the out-of-plane displacement component, ω is the natural frequency of plate in rad/sec, i is the complex number ($i^2 = -1$), and C_i are unknown constants. The transverse displacement W defined in Eq. (2) can be developed in Taylor's series as (Charbonneau and Lakis 2001)

$$W(x,y,t) = C_9 + C_{10}\frac{x}{A} + C_{11}\frac{y}{B} + C_{12}\frac{x^2}{2A^2} + C_{13}\frac{xy}{AB} + C_{14}\frac{y^2}{2B^2} + C_{15}\frac{x^3}{6A^3} + C_{16}\frac{x^2y}{2A^2B} + C_{17}\frac{xy^2}{2AB^2} + C_{18}\frac{y^3}{6B^3} + C_{19}\frac{x^3y}{6A^3B} + C_{20}\frac{xy^3}{6AB^3} \tag{3}$$

Finally, components of the displacement field are defined in the following form

$$\{U,V,W\}^T = [R]\{C\} \tag{4}$$

where $[R]$ is a matrix of order (3×20) given in Eq. (A.1) of Appendix and $\{C\}$ is the unknown constants' vector. These constants can be defined as a function of twenty degrees of freedom for the chosen element. Then, substituting the components of the constant vector into Eq. (4) leads to the following relationship

$$\{U,V,W\}^T = [R][A]^{-1}\{\delta\} \tag{5}$$

where $[A]^{-1}$ is a matrix of order (20×20) defined in Eq. (A.3) of Appendix and $\{\delta\}$ is the displacement vector of the finite element given in Eq. (A.4) of Appendix. Strain-displacement relations for the rectangular plates are given as (Sanders 1959)

$$\{\varepsilon_x, \varepsilon_y, 2\varepsilon_{xy}, \kappa_x, \kappa_y, \kappa_{xy}\}^T = \left\{\frac{\partial U}{\partial x}, \frac{\partial V}{\partial y}, \frac{\partial U}{\partial y} + \frac{\partial V}{\partial x}, -\frac{\partial^2 W}{\partial x^2}, -\frac{\partial^2 W}{\partial y^2}, -2\frac{\partial^2 W}{\partial x \partial y}\right\}^T \tag{6}$$

Introducing the displacement components defined by Eq. (5) into the deformation vector, one obtains the following equation that describes the deformation vector as a function of nodal displacements.

$$\{\varepsilon\} = [Q][A]^{-1}\{\delta\} \tag{7}$$

where $[Q]$ is a matrix of order (6×20) given in Eq. (A.5) of Appendix. The stress vector is defined by the following relation

$$\{\sigma\} = [P]\{\varepsilon\} \tag{8}$$

where $[P]$ is the elasticity matrix (6×6) whose components are given in Eq. (A.6) of Appendix. Using Eq. (5) to Eq. (8), the stiffness and mass matrices in the local co-ordinates of developed element are expressed by the following equations

$$[k]^e = [[A]^{-1}]^T \left(\int_0^{y_e} \int_0^{x_e} [Q]^T [P][Q] dx dy \right) [A]^{-1} \tag{9a}$$

$$[m]^e = \rho_s h [[A]^{-1}]^T \left(\int_0^{y_e} \int_0^{x_e} [R]^T [R] dx dy \right) [A]^{-1} \tag{9b}$$

where ρ_s is the structural density, h is the plate thickness and x_e and y_e are the element dimensions in X and Y directions, respectively (see Fig. 1).

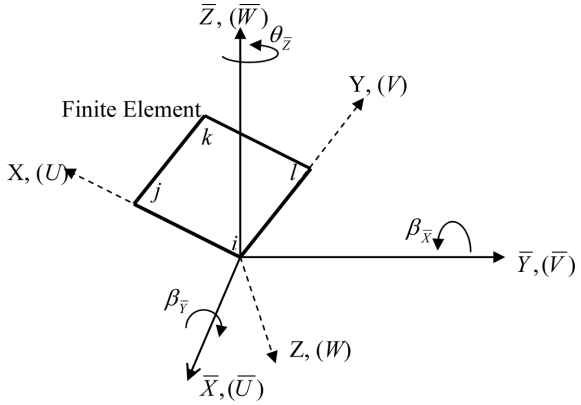

Fig. 2 Local and global co-ordinate systems of the structure

2.2 Transformation matrix

As shown in Fig. 2, the finite element is defined in its local co-ordinates, (X, Y, Z), which do not coincide with the global axes of the structure system $(\overline{X}, \overline{Y}, \overline{Z})$. Therefore, the local mass and stiffness matrices must be transformed to the global system before assembling into the global matrices that will describe the dynamic equations of motion. The displacement vector at each node in local co-ordinates may be defined as

$$\{\delta_i'\} = \{U_i, V_i, W_i, \partial W_i/\partial x, \partial W_i/\partial y, 0\}^T \tag{10}$$

The nodal displacement relationships between the local and global co-ordinates are expressed by the following equation

$$\{\delta_i'\} = \begin{bmatrix} \cos(X,\overline{X}) & \cos(X,\overline{Y}) & \cos(X,\overline{Z}) & 0 & 0 & 0 \\ \cos(Y,\overline{X}) & \cos(Y,\overline{Y}) & \cos(Y,\overline{Z}) & 0 & 0 & 0 \\ \cos(Z,\overline{X}) & \cos(Z,\overline{Y}) & \cos(Z,\overline{Z}) & 0 & 0 & 0 \\ 0 & 0 & 0 & -\cos(Y,\overline{Y}) & -\cos(Y,\overline{X}) & -\cos(Y,\overline{Z}) \\ 0 & 0 & 0 & \cos(X,\overline{Y}) & \cos(X,\overline{X}) & \cos(X,\overline{Z}) \\ 0 & 0 & 0 & \cos(Z,\overline{Y}) & \cos(Z,\overline{X}) & \cos(Z,\overline{Z}) \end{bmatrix} \{\overline{\delta}_i\} = [T_i]\{\overline{\delta}_i\} \tag{11}$$

where $[T_i]$ is a transformation matrix and $\{\overline{\delta}_i\}$ is the nodal displacement vector in global co-ordinates whose components are given as

$$\{\overline{\delta}_i\} = \{\overline{U}_i, \overline{V}_i, \overline{W}_i, \beta_{i,\overline{X}}, \beta_{i,\overline{Y}}, \theta_{i,\overline{Z}}\}^T \tag{12}$$

With application of Eq. (11) for all four nodes (i, j, k, l), one can obtain the following relation that describes the displacement components of each element in the global system.

$$\{\delta'\} = \begin{bmatrix} [T_i] & 0 & 0 & 0 \\ 0 & [T_j] & 0 & 0 \\ 0 & 0 & [T_k] & 0 \\ 0 & 0 & 0 & [T_l] \end{bmatrix} \{\bar{\delta}\} = [T^e]\{\bar{\delta}\} \tag{13}$$

where $\{\delta'\}$ and $\{\bar{\delta}\}$ are the displacement vectors of each element in local and global co-ordinates, respectively. Consequently, the stiffness and mass matrices of each element in global co-ordinates are determined by the following equations

$$\begin{aligned} [\bar{k}]^e &= [T^e]^T [k']^e [T^e] \\ [\bar{m}]^e &= [T^e]^T [m']^e [T^e] \end{aligned} \tag{14}$$

where $[k']^e$ and $[m']^e$ are the stiffness and mass matrices of the element, calculated using Eq. (9), and $[\bar{k}]^e$ et $[\bar{m}]^e$ are the corresponding matrices in global co-ordinates.

3. Fluid modeling

The fluid pressure applied on the structure can be expressed as a function of acceleration of the system (Lakis and Paidoussis 1971). The effects of a non-flowing fluid can be introduced by an added mass that increases the inertia of the coupled system (see Fig. 3). The set of equations of motion expressing the dynamic behaviour of a coupled fluid-structure system is defined by the following relation

$$[[M_s] - [M_f]]\{\ddot{\bar{\delta}}_T\} + [K_s]\{\bar{\delta}_T\} = \{0\} \tag{15}$$

where $[M_s]$ and $[K_s]$ are, respectively, the mass and stiffness matrices of the structure and $[M_f]$ is the added mass matrix representing the inertia force effect due to the presence of the fluid. $\{\bar{\delta}_T\}$ is the global displacement vector. The fluid-structure element in local coordinates is shown in Fig. 3. The boundary condition assures permanent contact at the fluid-structure interface. To develop the

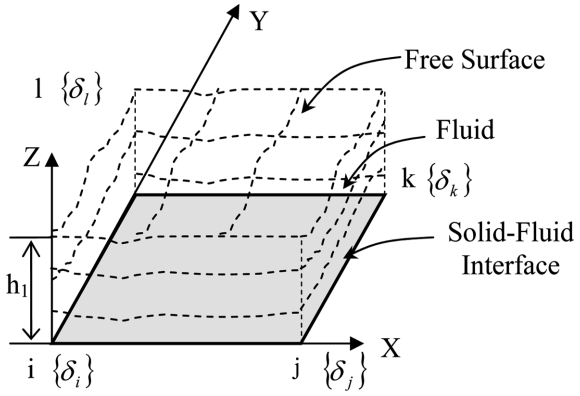

Fig. 3 Solid-fluid finite element in local co-ordinates X, Y, Z with free surface at ($Z = h_1$)

governing dynamic equations in the case of fluid-structure interaction, one assumes that the fluid is incompressible, non-viscous and irrotational. Therefore, the velocity potential function is used to determine the fluid force relations. Based on the aforementioned hypothesis the potential function, which satisfies the Laplace equation, is expressed in the Cartesian coordinate system as

$$\frac{\partial^2 \phi}{\partial x^2} + \frac{\partial^2 \phi}{\partial y^2} + \frac{\partial^2 \phi}{\partial z^2} = 0 \tag{16}$$

where ϕ is the velocity potential function. Using Bernoulli's equation, the fluid pressure at the solid-fluid interface may be expressed as

$$P|_{z=0} = -\rho_f \left.\frac{\partial \phi}{\partial t}\right|_{Z=0} \tag{17}$$

Using the mathematical technique of separation of variables, the velocity potential function is defined by the following relationship

$$\phi(x,y,z,t) = F(z)S(x,y,t) \tag{18}$$

At the fluid-structure interface, the impermeability conditions which assure permanent contact between the fluid and the structure are defined by

$$\left.\frac{\partial \phi}{\partial z}\right|_{Z=0} = \frac{\partial W}{\partial t} \tag{19}$$

where W is the transverse displacement of the plate in local co-ordinates and ϕ is the potential function. Using Eqs. (18) and (19), one can express the potential function as follows

$$\phi(x,y,z,t) = \frac{F(z)}{dF(0)/dz}\frac{\partial W}{\partial t} \tag{20}$$

To determine the potential function, one has to calculate the function $F(z)$. Substituting Eq. (20) into Eq. (16), one obtains the following differential equation

$$\frac{d^2F(z)}{dz^2} - \mu^2 F(z) = 0 \tag{21}$$

with: $\mu = \pi\sqrt{1/A^2 + 1/B^2}$

where A and B are plate lengths in the X and Y directions, respectively. The function $F(z)$ is obtained by solving the differential Eq. (21). The general solution of $F(z)$ is defined as

$$F(z) = A_1 e^{\mu z} + A_2 e^{-\mu z} \tag{22}$$

where, A_1 and A_2 are two unknown constants. Substituting Eq. (22) into Eq. (20), one obtains the following expression for the velocity potential function.

$$\phi(x,y,z,t) = \frac{(A_1 e^{\mu z} + A_2 e^{-\mu z})}{dF(0)/dZ}\frac{\partial W}{\partial t} \tag{23}$$

The potential function 'ϕ' must be verified for given boundary conditions at the fluid-structure interface ($Z = 0$) and the fluid extremity surfaces ($Z = h_1$ or $Z = h_2$) as well. The fluid boundary conditions are introduced separately for each element, which allows us to investigate the dynamic behaviour of totally or partially fluid-filled structures as well as submerged structures. The coupled fluid-structure system can take various forms.

3.1 Solid-fluid model bounded by free surface

Assuming that perturbations due to free surface motion of the fluid are insignificant, the following condition may be applied at the fluid free surface to the velocity potential (See Fig. 3)

$$\left.\frac{\partial\phi(x,y,z,t)}{\partial z}\right|_{Z=h_1} = -\frac{1}{g}\frac{\partial^2\phi}{\partial t^2} \tag{24}$$

where 'g' is acceleration due to gravity. Using Eqs. (19) and (24) we can calculate the constants A_1 and A_2 corresponding to this last boundary condition. Substituting these constants in Eq. (23) we obtain the following expression for the potential function

$$\phi(x,y,z,t) = \frac{1}{\mu}\left[\frac{e^{\mu z} + Ce^{-\mu(z-2h_1)}}{1 - Ce^{2\mu h_1}}\right]\frac{\partial W}{\partial t} \tag{25}$$

where

$$C = (g\mu - \omega^2)/(g\mu + \omega^2) \tag{26}$$

It is proven (Kerboua *et al*. 2005) that the coefficient C tends asymptotically toward (–1). This approximation is made in order to avoid non-linear eigenvalue problem. The corresponding dynamic pressure at the fluid-structure interface becomes

$$P = -\frac{\rho_f}{\mu}\left[\frac{1 + Ce^{2\mu h_1}}{1 - Ce^{2\mu h_1}}\right]\frac{\partial^2 W}{\partial t^2} = Z_{f1}\frac{\partial^2 W}{\partial t^2} \tag{27}$$

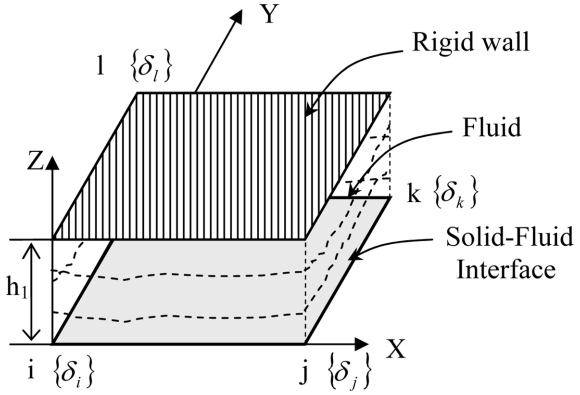

Fig. 4 Solid-fluid finite element, in a local co-ordinate *X, Y, Z*, bounded by a rigid wall

3.2 Plate-fluid model bounded by a rigid wall

The boundary condition at the upper surface of the fluid represented in Fig. 4 was studied by Lamb (1920) and referred to as the null-frequency condition. This rigid wall boundary condition is expressed as

$$\left.\frac{\partial \phi}{\partial z}\right|_{Z=h_1} = 0 \tag{28}$$

Similarly, by introducing Eq. (23) into relations (19) and (28), we obtain the following expression for the velocity potential as follows

$$\phi(x,y,z,t) = \frac{1}{\mu}\left[\frac{e^{\mu(z-2h_1)} + e^{-\mu z}}{e^{-2\mu h_1} - 1}\right]\frac{\partial W}{\partial t} \tag{29}$$

The dynamic pressure at the fluid-structure interface for this case is determined as

$$P = -\frac{\rho_f}{\mu}\left[\frac{e^{-2\mu h_1} + 1}{e^{-2\mu h_1} - 1}\right]\frac{\partial^2 W}{\partial t^2} = Z_{f2}\frac{\partial^2 W}{\partial t^2} \tag{30}$$

3.3 Fluid-solid element for the parallel/and radial plates

In case of a rectangular reservoir, (see Fig. 5) as well as in case of parallel plates (Figs. 6 and 7) and radial plates (Fig. 8), the fluid acts on the inner surface of elastic walls. These components can vibrate according to in-phase or out-of-phase modes with each other. The impermeability condition for each element of this fluid-structure system remains unchanged, while the boundary conditions vary in terms of vibrational modes. Both cases are discussed in the following subsections.

3.3.1 In-phase vibrational mode of parallel plates

In the case of in-phase vibration of two elastic walls shown in Fig. 5, the boundary condition at fluid level $Z = h_1$ is defined by the following relation.

$$\left.\frac{\partial \phi}{\partial z}\right|_{Z=h_1} = \frac{\partial W}{\partial t} \tag{31}$$

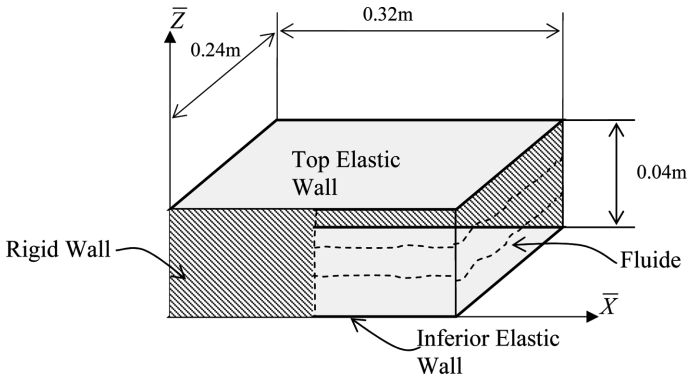

Fig. 5 Fluid-filled rectangular reservoir with vertical rigid walls

Substituting Eq. (23) simultaneously into Eqs. (19) and (31), one obtains the constants A_1 and A_2. Introducing these constants into Eq. (23), one can express the following velocity potential function

$$\phi(x,y,z,t) = \frac{1}{\mu}\left[\frac{(1-e^{-\mu h_1})e^{\mu z} + (1-e^{\mu h_1})e^{-\mu z}}{e^{\mu h_1} - e^{\mu h_1}}\right]\frac{\partial W}{\partial t} \tag{32}$$

Substituting relation (32) into Eq. (17), the dynamic pressure is expressed as

$$P = -\frac{\rho_f}{\mu}\left[\frac{2-e^{-\mu h_1} - e^{\mu h_1}}{e^{\mu h_1} + e^{-\mu h_1}}\right]\frac{\partial^2 W}{\partial t^2} = Z_{f3}\frac{\partial^2 W}{\partial t^2} \tag{33}$$

When the two walls are radials (see Fig. 8), the term on the right-hand side of Eq. (31) to Eq. (33) must be multiplied by a factor of $\cos(\alpha)$, where α is the angle between two adjacent walls.

3.3.2 Out-of-phase vibrational modes of parallel plates

In the case of out-of-plane vibrational modes, the boundary condition at the fluid level $Z = h_1$ is given by

$$\left.\frac{\partial \phi}{\partial z}\right|_{Z=h_1} = -\frac{\partial W}{\partial t} \tag{34}$$

Substituting Eq. (23) into Eqs. (19) and (34), the constants A_1 and A_2 can be calculated. Introducing these constants into Eq. (23) results in the following expression for the velocity potential function

$$\phi(x,y,z,t) = \frac{1}{\mu}\left[\frac{(1+e^{\mu h_1})e^{\mu z} + (e^{\mu h_1} + e^{2\mu h_1})e^{-\mu z}}{1-e^{2\mu h_1}}\right]\frac{\partial W}{\partial t} \tag{35}$$

The fluid pressure at the fluid-structure interface is determined by substitution of the potential function (35) into Eq. (17)

$$P = -\frac{\rho_f}{\mu}\left[\frac{1+2e^{\mu h_1} + e^{2\mu h_1}}{1-e^{2\mu h_1}}\right]\frac{\partial^2 W}{\partial t^2} = Z_{f4}\frac{\partial^2 W}{\partial t^2} \tag{36}$$

When both walls are elastic and radial (Fig. 8), the right-hand terms in Eq. (34) to Eq. (36) must be multiplied by a factor of $\cos(\alpha)$, where α is the angle between two adjacent walls.

4. Calculation of fluid-induced force

The fluid-induced force vector in the local coordinate system can be expressed as

$$\{F\}^e = \int_A [[A]^{-1}]^T [R]^T \{P_f\}\, dA \tag{37}$$

where $\{P_f\}$ is the tensor of fluid pressure acting on the fluid-structure element. P is the only non-zero component in the pressure tensor $\{P_f\}$. Replacing the transverse displacement component of Eq. (5) into fluid pressure expressions which varies depending on the case in question (see Eqs. (27), (30), (33) and (36)) one gets the following expression for the fluid pressure acting on the structure

$$\{P_f\} = Z_{fi}[R_f][A]^{-1}\{\ddot{\delta}\} \tag{38}$$

where Z_{fi} ($i = 1, 4$), depends on the fluid boundary conditions (see Eqs. (27), (30), (33) and (36)) and $[R_f]$ is matrix of order (3×20) given in Eq. (A.2) of Appendix. Replacing the pressure expression (38) into Eq. (37), the force vector for each element is given by

$$\{F\}^e = Z_{fi}\int_A [[A]^{-1}]^T [R]^T [R_f][A]^{-1} dA\{\ddot{\delta}\} = [m_f]^e\{\ddot{\delta}\} \tag{39}$$

where dA is an elementary surface and $[m_f]^e$ is the fluid mass matrix of order (20×20) corresponding to one finite element in local co-ordinate system.

The pressure expressed by Eqs. (27), (30), (33) and (36) and the velocity potential expressed by Eqs. (25), (29), (32) and (35) describe the effect of the column of fluid (either above or below) on a single finite element of the elastic structure. The fluid effect on the entire structure is described by the global system of equations by introducing the global matrix of added mass generated by the fluid pressure. This global matrix is created by assembling the added mass matrices of each element.

For X and Y in the finite element domain, the potential and pressure at the interface are coupled by the transverse movement of the plate $W(x, y, t)$ and its derivatives. Eq. (20) describes the function in terms of this transverse movement of the structure $W(x, y, t)$ which itself varies as a function of structure geometry and time. Therefore, the movement of the liquid at any point on the interface (including the boundaries X and Y) is intimately linked to the movement of the edges of the elastic structure. The boundary conditions in X and Y are those of the transverse movement of the plate; $W(x, y, t)$. X and Y are limited at the medium of the interaction fluid-solid because the concept of the method eliminates the need for an analytical solution for the integrity of the fluid-solid medium.

5. Calculation of $[K_s]$, $[M_s]$ and $[M_f]$ and eigenvalue problem

The structure is subdivided into a set of quadrilateral elements. The stiffness and mass (solid and fluid) matrices are determined for each element in its local co-ordinates. Then, they are transferred to the global system of co-ordinates in order to assemble the global matrices defined in Eq. (15).

We will assume that

$$\{\bar{\delta}_T\} = \{\bar{\delta}_{0T}\}e^{i\omega t} \tag{40}$$

where $\{\bar{\delta}_T\}$ is the global displacement vector, ω is the natural frequency of system (rad/sec); and $\{\bar{\delta}_{0T}\}$ is the global displacement amplitude vector for each mode. Substituting Eq. (40) into Eq. (15) leads to the following eigenvalue problem

$$Det[[K_s] - \omega^2[M_s - M_f]] = 0 \tag{41}$$

Solution of this system results in the natural frequencies and mode shapes of the structure.

6. Results and discussions

Many works have been carried out to study the axisymetric structures, such as cylindrical shells and circular plates. Research works dealing with hydro-elastic analysis of structures composed of plates and shells components are rare. The developed fluid-solid element in this work is used to study the hydro-elastic behaviour of:

a. Two identical parallel plates in interaction with a bounded fluid
b. A set of plates fixed at a rigid wall
c. A set of plates used in a heat exchanger
d. A set of radial plates
e. A set of plates fixed at an elastic wall

a. The first structure is a fluid-filled rectangular reservoir that was studied by Jeong *et al.* (2004). The vessel dimensions are given in Fig. 5 and the plate thickness is h = 2 mm. The physical properties of the material are as follows: Young's modulus = 69 GPa, Poisson's ratio = 0.3 and mass density = 2700 kg/m^3. Water is used as the fluid in contact with plates, having a density of 1000 kg/m^3. The lateral walls of the reservoir are rigid. The top and base plates are elastic and fixed to the lateral walls. The elastic plates vibrate in the presence of fluid in both in-phase and out-of-phase modes. Some vibration modes are not permitted in order to not violate the mass conservation of incompressible fluid (Jeong *et al.* 2004). Table 1 lists natural frequencies for in-phase modes of the two plates coupled with the movement of an incompressible fluid. The results presented in Table 1, show an excellent agreement between our presented theory and that of Jeong *et al.* (2004). The natural frequencies of the two parallel plates coupled with an incompressible fluid and vibrating in out-of-phase mode (0,1) are listed in Table 2. Only the frequency corresponding to the mode (0,1) is presented since it preserves the mass conservation that was also met by Jeong *et al.* (1998) in the analysis of two circular plates coupled with fluid. Regarding the dynamic analysis of two identical rectangular plates in interaction with fluid as studied by Jeong *et al.* (2004), the displacement function for the in-phase and out-of-phase modes is not the same. Another displacement function is adopted so that the mode shape compensates for the change of fluid volume in the Z direction. To

Table 1 In-phase vibrational frequencies (Hz) of a fluid-filled reservoir

Mode number (n, m)	Jeong *et al.* (2004)	Present theory
(0,0)	113.3	112.9
(0,1)	192.5	188.7
(1,0)	272.4	265.6
(0,2)	326.5	314.0
(1,1)	348.4	332.9
(1,2)	479.6	447.7
(0,3)	516.1	485.6
(2,0)	525.9	498.2

Table 2 Out-of-phase vibration frequencies (Hz) of a fluid-filled reservoir

Mode number (n, m)	Jeong *et al.* (2004)	Present theory
(0,1)	61.2	66.5

calculate the other modes one must therefore impose some conditions in the displacement field such that the assumption for incompressible fluid is respected. This problem arises in closed structures completely filled with an incompressible fluid.

b. Some structures are composed of a set of identical parallel or radial plates that are in interaction with the fluid. An example is MTR-type flat-plate fuel elements in nuclear reactors. If the height of fluid between the plates is relatively low, the fluid transports the kinetic energy from one plate to another. Therefore, one studies the case of three parallel plates fixed to a rigid wall as shown in Fig. 6. The material properties are as follows: Young's modulus = 69 GPa, Poisson's ratio = 0.3 and mass density = 2700 kg/m^3. When the system is submerged in a large reservoir, every plate experiences a different pressure at its two sides caused by the fluid on both top and bottom of the plate. In addition, the plates vibrate according to in-phase or out-of-phase modes. For each mode, there is a distinct fluid pressure that is presented in Table 3. Among several possible combinations, one distinguishes three modes of vibration of the system. The remaining cases are only repetitions of one of the three modes. Table 4 presents vibration frequencies according to the three distinct modes of plate. From these results, we note that the dynamic behaviour of this system can be studied by considering only one internal plate that vibrates according to out-of-phase mode relatively to the two others since this mode provides the lowest frequency.

c. Assembled parallel plates are often used in different industrial sectors. Fig. 7 shows a part of a structural system composed of a set of thin plates, each with two parallel sides fixed to lateral rigid

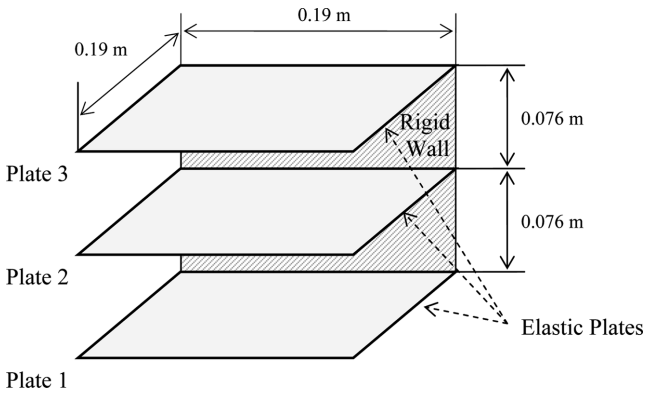

Fig. 6 A set of parallel plates fixed at a rigid wall and totally submerged in fluid

Table 3 Number of equations for expressing the pressure corresponding to each vibration mode of submerged plates (see Fig. 6)

Vibrational mode	Plate 1		Plate 2		Plate 3	
	Upper pressure	Lower pressure	Upper pressure	Lower pressure	Upper pressure	Lower pressure
Three plates vibrating in-phase	(33)	(30)	(33)	(33)	(27)	(33)
Plate (2) is out-of-phase with plates (1) and (3)	(36)	(30)	(36)	(36)	(27)	(36)
Plate (2) is out-of-phase with plate (3) and is in-phase with plate (1)	(33)	(30)	(36)	(33)	(27)	(36)

Table 4 Vibration frequencies (Hz) of a set of three plates fixed to rigid wall (see Fig. 6)

Mode number	Three submerged plates vibrating in-phase	Plate (2) is out-of-phase with plates (1) and (3)	Plate (2) is out-of-phase with plate (3) and is in-phase with plate (1)
1	12.3	9.7	10.5
2	12.3	10.5	11.1
3	13.4	15.7	12.3
4	30.1	23.8	25.7
5	30.1	25.7	27.3
6	32.8	38.5	30.1
7	75.9	60.0	64.6
8	75.9	64.6	68.7
9	82.7	75.7	75.9
10	95.7	81.5	81.5

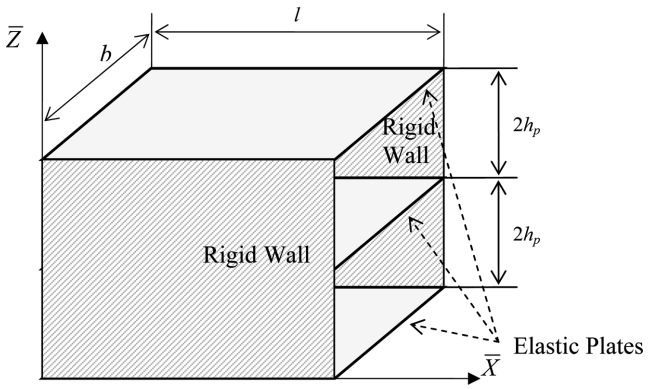

Fig. 7 A set of parallel plates with two parallel sides fixed to lateral rigid walls $\eta = \rho_f b/\rho_s h = 1$, $\zeta = l/b = 0.5$; $\psi = h_p/b = 0.05$

walls. All plates have the same properties and they are distributed uniformly. Guo and Paidoussis (2000) studied an identical system submitted to a flowing fluid in channels formed by rectangular plates. They only considered the out-of-phase vibration modes since they are most problematic. Here, it is assumed that the fluid velocity is null and only the inertia force due to the fluid is taken into account. A dimensionless frequency parameter is defined by the following expression

$$\omega = (1/b)^2 \sqrt{K/(\rho_s h_p)}\,\overline{\omega} \tag{42}$$

where K is the bending rigidity, ω is the natural frequency in rad/sec, $\overline{\omega}$ is the dimensionless natural frequency. 'h_p', 'b', and 'l' are represented in Fig. 7. To put the results in the non-dimensional form, the following parameters are defined

$$\eta = \rho_f b/\rho_s h = 1; \quad \zeta = l/b = 0.5; \quad \psi = h_p/b = 0.05 \tag{43}$$

where η is the mass ratio. ζ and ψ are geometric ratios.

Table 5 Non-dimensional out-of-phase vibration frequencies (see Fig. 7)

Mode number	Present theory	Guo and Paidoussis (2000)
1	16.3	16.6
2	26.5	32.5
3	45.0	48.5

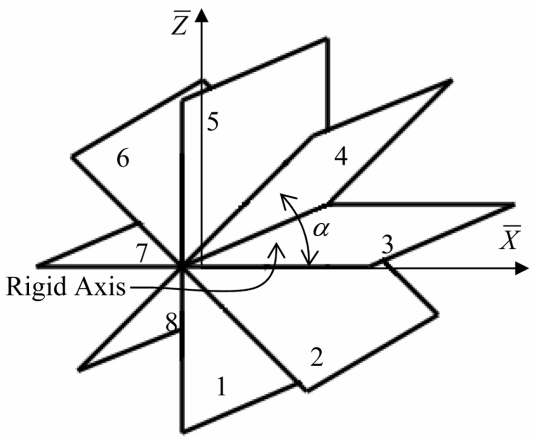

Fig. 8 A structural system composed of n radial plates welded to a common rigid axis

The structure is discretized into a number of quadrilateral elements. All nodal degrees of freedom belonging to the rigid walls are eliminated. The pressure applied on the middle plate is the sum of the calculated pressure acting on the upper and lower surfaces of the plate. Because of geometrical symmetry the pressure applied on the top and bottom plates is the same. It is for this reason that analysis of a set of plates reverts to the study of only one plate subjected to the calculated pressure on the side walls in an out-of-phase vibration mode. Table 5 lists the non-dimensional natural frequencies of the fluid-structure model for the case of non-flowing fluid along with the corresponding results calculated by Guo and Paidoussis (2000).

d. the developed solid-fluid model was used to study the dynamic behaviour of a system composed of several radial plates having one side of each plate welded to a rigid axis as shown in Fig. 8. The angle between each pair of plates is 45 degrees. All plates have the same geometrical dimensions and mechanical properties which are given as follows:

B = 0.655 m, A = 0.2016 m, h = 9.36 mm, E = 207 GPa, ρ_s = 7850 kg/m^3 and ν = 0.3

In this structural model, the fluid level on the top and bottom of the plates varies from one element to another. Considering the axial symmetry of the system and the uniform distribution of the plates in the circumferential direction, dynamic analysis of such a system comes back to study only one plate that vibrates according to three different modes in relation with its neighbouring plates (Guo and Paidoussis 2000). The fluid pressures applied on plate 2, corresponding to each mode of vibration are listed in Table 6. Natural frequencies of this structure without fluid and when totally submerged in a large water reservoir according to the three distinct modes are enumerated in Table 7.

It is important to note that the dynamic analysis of a set of parallel or radial plates can only be reduced to the dynamic analysis of one plate when all plates have the same dimensions and the

Table 6 Number of equations for expressing the pressure corresponding to each vibration mode of radial submerged plates (see Fig. 8)

Vibrational mode	Plate 2	
	Upper pressure	Lower pressure
Three plates vibrating in-phase	Eq. (33) $\cos\alpha$	Eq. (33) $\cos\alpha$
Plate (2) is out-of-phase with plates (1) and (3)	Eq. (36) $\cos\alpha$	Eq. (36) $\cos\alpha$
Plate (2) is out-of-phase with plate (3) and is in-phase with plate (1)	Eq. (36) $\cos\alpha$	Eq. (33) $\cos\alpha$

Table 7 Vibration frequencies (Hz) of radial plates (see Fig. 8)

Mode number	In air	In fluid		
		Three plates vibrating in-phase	Plate (2) is out-of-phase with plates (1) and (3)	Plate (2) is out-of-phase with plate (3) and is in-phase with plate (1)
1	199.1	140.0	116.4	126.5
2	242.6	170.6	141.6	154.0
3	361.9	255.1	210.7	229.5
4	558.1	394.3	323.6	353.4
5	851.5	602.6	491.9	538.4
6	1243.6	885.1	683.0	773.0
7	1251.1	917.6	699.1	780.6
8	1311.6	957.9	732.2	815.0
9	1440.9	1056.7	785.3	889.3
10	1679.4	1233.8	911.2	1034.2

Table 8 Vibration frequencies (Hz) of a set of three plates fixed to elastic wall

Mode number	Present theory (in vacuum)	ANSYS (in vacuum)	Three submerged plates vibrating in-phase
1	28,71	28,71	7,58
2	37,73	37,739	10.49
3	ND	52,6	ND
4	83,35	84,98	29.59
5	97,74	93,29	54.06
6	105,3	105,26	57.58
7	ND	134	ND
8	147	150	59.6
9	174,7	174,4	68.09
10	186	ND	74.25
11	246,4	245,31	92.17
12	290,7	289,21	92.93
13	317,8	316,09	93.38
14	357,4	358,94	100
15	358,8	360,57	104.7

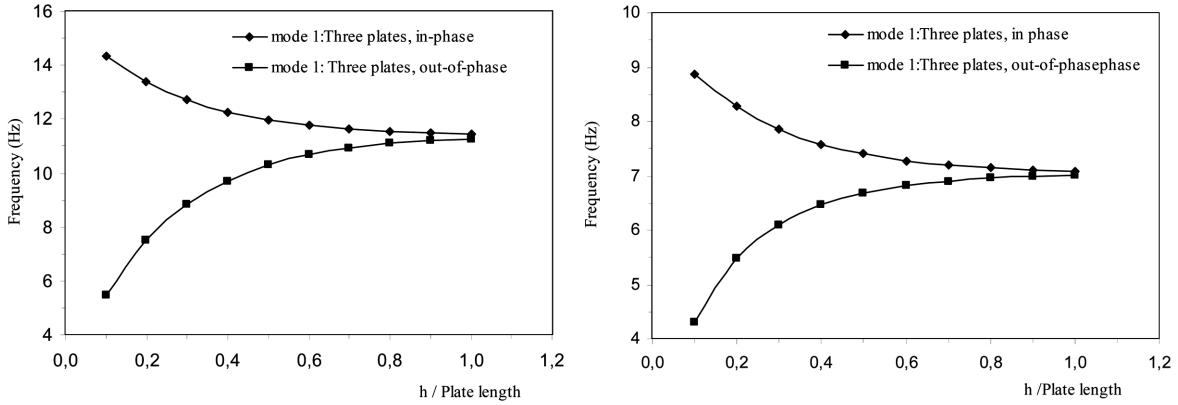

(A) Three plates fixed at a rigid wall **(B) Three plates fixed at an elastic wall**

Fig. 9 In-phase and out-of-phase vibration frequencies (Hz) of a set of parallel plates as a function of fluid level to plate length ratio

same mechanical properties. In addition, the fluid height has to be even between every pair of plates and the axis (Fig. 8) or the wall (Fig. 6) that attaches all plates together must be rigid.

e. The dynamic behaviour of the system represented in Fig. 6 is studied while assuming that the vertical wall plate is elastic and no displacement condition is imposed (free-free). In Table 8, we have the natural frequencies of the system calculated without fluid by our program and by ANSYS software as well as the frequencies corresponding to in-phase mode vibration of the three plates when the system is completely submerged in a reservoir of infinite size. We note that the frequencies are not repeated, which is contrary to the case of plates clamped to a rigid wall (see Fig. 6), since this repetition is due to the effects of the boundary conditions. In this case, it is necessary to study all the possible combinations of in-phase and out-of-phase modes of the plates.

When the system composed of parallel plates fixed to elastic or rigid wall (see Fig. 6) is submerged in a large reservoir, the fluid height between the plates is a very important parameter. Resonance frequency variation as a function of fluid height to plate length ratio (h_1/Length) for the structural systems is plotted in Fig. 9 when the three plates vibrate according to in-phase and out-of-phase modes. We note that when we increase the fluid-height between the plates the in-phase frequency decreases whereas the out-of-phase frequency increases. This behaviour was underlined by Jeong 2003 in the case of two circular plates and that of two rectangular plates (Jeong *et al.* 2004) in interaction with the fluid. As shown in Fig. 9, the fluid height at which there is no difference between the in-phase and out-of-phase frequencies is equal to the plate length.

7. Conclusions

A hybrid element is developed for dynamic analysis of coupled fluid-structure systems such as parallel plate assemblies or radial plates. The structure may be empty, partially or completely filled with fluid or submerged in a liquid. The structural mass and stiffness matrices are determined by exact analytical integration. The in-plane and out-of-plane displacement components are modelled using bilinear polynomials and exponential functions, respectively. The velocity potential and

Bernoulli's equation are adopted to express the fluid pressure acting on the structure. The product of the pressure expression and the developed structural shape function is integrated over the structure-fluid interface to assess the virtual added mass due to the fluid.

It is noted that increasing the fluid height results in a reduction of frequencies for in-phase modes and an increase of frequencies for out-of-phase modes. When the height of the fluid is equal to the length of the plate, there is no difference between the in-phase and out-of-phase modes. This means that the fluid transports the kinetic energy from one plate to another along a limited distance.

While calculating frequencies and vibration modes of several structures having different geometries, it is proven that the developed computational approach is a powerful and reliable tool for dynamic analysis of a variety of plate and shell structures. While comparing our results with those of other researchers (either analytical or experimental works) we can conclude that the developed fluid-structure element generates satisfactory results. This hybrid element can be applied for vibration analysis of non-uniform structures supported by any combination of various boundary conditions.

The important result of this work was the confirmation of the applicability of this element to represent the hydro-elastic behaviour of different structures. The next step is to apply this element to study the effect of other aspects such as material and structural discontinuity, and structural curvature on the dynamic responses of coupled fluid-structure systems.

References

Amabili, M. and Dalpiaz, G. (1995), "Breathing vibrations of a horizontal circular cylindrical tank shell, partially filled with liquid", *J. Vib. Acoust.*, **117**(2), 187-191.

Amabili, M. and Kwak, M.K. (1999), "Vibration of circular plates on a free fluid surface: Effect of surface waves", *J. Sound Vib.*, **226**(3), 407-424.

Bauer, H.F. (1981), "Hydroelastic vibrations in a rectangular container", *Int. J. Solids Struct.*, **17**(7), 639-652.

Berry, J.G. and Reissner, E. (1958), "The effect of an internal compressible fluid column on the breathing vibrations of a thin pressurized cylindrical shell", *J. Aerospace Sci.*, **25**, 288-294.

Charbonneau, E. and Lakis, A.A. (2001), "Semi-analytical shape functions in the finite element analysis of rectangular plates", *J. Sound Vib.*, **242**(3), 427-443.

Cheung, Y.K. and Zhou, D. (2000), "Coupled vibratory characteristics of a rectangular container bottom plate", *J. Fluids Struct.*, **14**(3), 339-357.

Cheung, Y.K. and Zhou, D. (2002), "Hydroelastic vibration of a circular container bottom plate using the Galerkin method", *J. Fluids Struct.*, **16**(4), 561-580.

Ding, Z. and Weiqing, L. (2007), "Hydroelastic vibrations of flexible rectangular tanks partially filled with liquid", *Int. J. Numer. Meth. Eng.*, **71**, 149-174.

Fu, Y. and Price, W.G. (1987), "Interactions between a partially or totally immersed vibrating cantilever plate and the surrounding fluid", *J. Sound Vib.*, **118**(3), 495-513.

Guo, C.Q. and Paidoussis, M.P. (2000), "Analysis of hydroelastic instabilities of rectangular parallel-plate assemblies", *J. Press. Vess. -T. ASME.*, **122**(4), 502-508.

Jain, R.K. (1974), "Vibration of fluid-filled, orthotropic cylindrical shells", *J. Sound Vib.*, **37**(3), 379-388.

Jeong, K.H. (2003), "Free vibration of two identical circular plates coupled with bounded fluid", *J. Sound Vib.*, **260**(4), 653-670.

Jeong, K.H., Yoo, G.H.Y. and Lee, S.C. (2004), "Hydroelastic vibration of two identical rectangular plates", *J. Sound Vib.*, **272**(3-5), 539-555.

Jeong, K.H., Kim, T.W., Choi, S. and Park, K.B. (1998), "Free vibration analysis of two circular disks coupled with fluid", Proceeding of San Diego, CA, USA.

Kerboua, Y., Lakis, A.A., Thomas, M. and Marcouiller, L. (2005), "Comportement dynamique des plaques rectangulaires submergées", Ecole polytechnique de Montréal, EPM-RT-2005-05.
Kim, M.C. and Lee, S.S. (1997), "Hydroelastic analysis of rectangular tank", Proceeding of The aerospace corporation El Segundo, California 90245.
Kwak, M.K. (1994), "Vibration of circular membranes in contact with water", *J. Sound Vib.*, **178**(5), 688-690.
Kwak, M.K. (1997), "Hydroelastic vibration of circular plates", *J. Sound Vib.*, **201**(3), 293-303.
Kwak, M.K. and Han, S.B. (2000), "Effect of fluid depth on the hydroelastic vibration of free-edge circular plate", *J. Sound Vib.*, **230**(1), 171-185.
Lakis, A.A. and Paidoussis, M.P. (1971), "Free vibration of cylindrical shells partially filled with liquid", *J. Sound Vib.*, **19**(1), 1-15.
Lamb, H. (1920), "On the Vibrations of an Elastic Plate in Contact with Water", *Proc. Royal Society of London.*, **98**(690), 205-216.
Lamb, H. (1945), "Hydrodynamics", Sixsth edition, Dover Publication, New York.
Lindholm, U.S., Kana, D.D. and Abramson, H.N. (1962), "Breathing vibrations of circular cylindrical shell with internal liquid", *J. Aerospace Sci.*, **29**(9), 1052-1059.
Lindholm, U.S., Kana, D.D., Chu, W.H. and Abramson, H.N. (1965), "Elastic vibration characteristics of cantilever plates in water", *J. Ship Res.*, **9**(1), 11-22.
Rayleigh, L. (1945), *Theory of Sound*, Second Edition Dover New York.
Sanders, J.L. (1959), *An Improved First Approximation Theory for Thin Shells* NASA, TR-R24.
Santanu, M. and Sinhamahapatra, K.P. (2005), "Coupled slosh dynamics of liquid filled containers using pressure based finite element method", Proceeding of Exploring Innovation in Education and Research, Taiwan.
Selmane, A. and Lakis, A.A. (1997), "Vibration analysis of anisotropic open cylindrical shells subjected to a flowing fluid", *J. Fluid. Struct.*, **11**(1), 111-134.

Appendix

Matrix R (3 × 20)

$$[R] = \begin{bmatrix} 1 & x & y & xy & 0 & 0 & 0 & 0 & 0 & 0 & 0 & 0 & 0 & 0 & 0 & 0 & 0 & 0 & 0 & 0 \\ 0 & 0 & 0 & 0 & 1 & x & y & xy & 0 & 0 & 0 & 0 & 0 & 0 & 0 & 0 & 0 & 0 & 0 & 0 \\ 0 & 0 & 0 & 0 & 0 & 0 & 0 & 0 & 1 & \frac{x}{A} & \frac{y}{B} & \frac{x^2}{2A^2} & \frac{xy}{AB} & \frac{y^2}{2B^2} & \frac{x^3}{6A^3} & \frac{x^2y}{2A^2B} & \frac{xy^2}{2AB^2} & \frac{y^3}{6B^3} & \frac{x^3y}{6A^3B} & \frac{xy^3}{6AB^3} \end{bmatrix} \quad \text{(A.1)}$$

Matrix R_f (3 × 20)

$$[R_f] = \begin{bmatrix} 0 & 0 & 0 & 0 & 0 & 0 & 0 & 0 & 0 & 0 & 0 & 0 & 0 & 0 & 0 & 0 & 0 & 0 & 0 & 0 \\ 0 & 0 & 0 & 0 & 0 & 0 & 0 & 0 & 0 & 0 & 0 & 0 & 0 & 0 & 0 & 0 & 0 & 0 & 0 & 0 \\ 0 & 0 & 0 & 0 & 0 & 0 & 0 & 0 & 1 & \frac{x}{A} & \frac{y}{B} & \frac{x^2}{2A^2} & \frac{xy}{AB} & \frac{y^2}{2B^2} & \frac{x^3}{6A^3} & \frac{x^2y}{2A^2B} & \frac{xy^2}{2AB^2} & \frac{y^3}{6B^3} & \frac{x^3y}{6A^3B} & \frac{xy^3}{6AB^3} \end{bmatrix} \quad \text{(A.2)}$$

Matrix A^{-1} (20 × 20)

$$[A]^{-1} = \begin{bmatrix} 1 & 0 & 0 & 0 & 0 & 0 & 0 & 0 & 0 & 0 & 0 & 0 & 0 & 0 & 0 & 0 & 0 & 0 & 0 & 0 \\ -\frac{A}{x_e} & 0 & 0 & 0 & 0 & \frac{A}{x_e} & 0 & 0 & 0 & 0 & 0 & 0 & 0 & 0 & 0 & 0 & 0 & 0 & 0 & 0 \\ -\frac{B}{y_e} & 0 & 0 & 0 & 0 & 0 & 0 & 0 & 0 & 0 & 0 & 0 & 0 & 0 & 0 & \frac{B}{y_e} & 0 & 0 & 0 & 0 \\ \frac{AB}{x_e y_e} & 0 & 0 & 0 & 0 & -\frac{AB}{x_e y_e} & 0 & 0 & 0 & 0 & -\frac{AB}{x_e y_e} & 0 & 0 & 0 & 0 & -\frac{AB}{x_e y_e} & 0 & 0 & 0 & 0 \\ 0 & 1 & 0 & 0 & 0 & 0 & 0 & 0 & 0 & 0 & 0 & 0 & 0 & 0 & 0 & 0 & 0 & 0 & 0 & 0 \\ 0 & -\frac{A}{x_e} & 0 & 0 & 0 & 0 & \frac{A}{x_e} & 0 & 0 & 0 & 0 & 0 & 0 & 0 & 0 & 0 & 0 & 0 & 0 & 0 \\ 0 & -\frac{B}{y_e} & 0 & 0 & 0 & 0 & 0 & 0 & 0 & 0 & 0 & 0 & 0 & 0 & 0 & 0 & \frac{B}{y_e} & 0 & 0 & 0 \\ 0 & \frac{AB}{x_e y_e} & 0 & 0 & 0 & 0 & -\frac{AB}{x_e y_e} & 0 & 0 & 0 & 0 & \frac{AB}{x_e y_e} & 0 & 0 & 0 & 0 & -\frac{AB}{x_e y_e} & 0 & 0 & 0 \\ 0 & 0 & 1 & 0 & 0 & 0 & 0 & 0 & 0 & 0 & 0 & 0 & 0 & 0 & 0 & 0 & 0 & 0 & 0 & 0 \\ 0 & 0 & 0 & A & 0 & 0 & 0 & 0 & 0 & 0 & 0 & 0 & 0 & 0 & 0 & 0 & 0 & 0 & 0 & 0 \\ 0 & 0 & 0 & 0 & B & 0 & 0 & 0 & 0 & 0 & 0 & 0 & 0 & 0 & 0 & 0 & 0 & 0 & 0 & 0 \\ 0 & 0 & -\frac{6A^2}{x_e^2} & -\frac{4A^2}{x_e} & 0 & 0 & 0 & \frac{6A^2}{x_e^2} & -\frac{2A^2}{x_e} & 0 & 0 & 0 & 0 & 0 & 0 & 0 & 0 & 0 & 0 & 0 \\ 0 & 0 & -\frac{AB}{x_e y_e} & -\frac{AB}{y_e} & -\frac{AB}{x_e} & 0 & 0 & \frac{AB}{x_e y_e} & 0 & \frac{AB}{x_e} & 0 & 0 & -\frac{AB}{x_e y_e} & 0 & 0 & 0 & 0 & \frac{AB}{x_e y_e} & \frac{AB}{y_e} & 0 \\ 0 & 0 & -\frac{6B^2}{y_e^2} & 0 & -\frac{4B^2}{y_e} & 0 & 0 & 0 & 0 & 0 & 0 & 0 & 0 & 0 & 0 & 0 & 0 & \frac{6B^2}{y_e^2} & 0 & -\frac{2B^2}{y_e} \\ 0 & 0 & -\frac{12A^3}{x_e^3} & -\frac{6A^3}{x_e^2} & 0 & 0 & 0 & -\frac{12A^3}{x_e^3} & \frac{6A^3}{x_e^2} & 0 & 0 & 0 & 0 & 0 & 0 & 0 & 0 & 0 & 0 & 0 \\ 0 & 0 & \frac{6BA^2}{y_e x_e^2} & \frac{4BA^2}{y_e x_e} & 0 & 0 & 0 & -\frac{6BA^2}{y_e x_e^2} & \frac{2BA^2}{y_e x_e} & 0 & 0 & 0 & \frac{6BA^2}{y_e x_e^2} & -\frac{2BA^2}{y_e x_e} & 0 & 0 & 0 & -\frac{6BA^2}{y_e x_e^2} & -\frac{4BA^2}{y_e x_e} & 0 \\ 0 & 0 & -\frac{6AB^2}{x_e y_e^2} & 0 & -\frac{4AB^2}{y_e x_e} & 0 & 0 & -\frac{6AB^2}{x_e y_e^2} & 0 & -\frac{4AB^2}{y_e x_e} & 0 & 0 & \frac{6AB^2}{x_e y_e^2} & 0 & -\frac{2AB^2}{y_e x_e} & 0 & 0 & -\frac{6AB^2}{x_e y_e^2} & 0 & -\frac{2AB^2}{y_e x_e} \\ 0 & 0 & -\frac{12B^3}{y_e^3} & 0 & \frac{6B^3}{y_e^2} & 0 & 0 & 0 & 0 & 0 & 0 & 0 & 0 & 0 & 0 & 0 & 0 & -\frac{12B^3}{y_e^3} & 0 & -\frac{6B^3}{y_e^2} \\ 0 & 0 & -\frac{12BA^3}{y_e x_e^3} & -\frac{6BA^3}{y_e x_e^3} & 0 & 0 & 0 & \frac{12BA^3}{y_e x_e^3} & -\frac{6BA^3}{y_e x_e^2} & 0 & 0 & 0 & -\frac{12BA^3}{y_e x_e^3} & \frac{6BA^3}{y_e x_e^2} & 0 & 0 & 0 & \frac{12BA^3}{y_e x_e^3} & \frac{12BA^3}{y_e x_e^2} & 0 \\ 0 & 0 & -\frac{12AB^3}{x_e y_e^3} & 0 & -\frac{6AB^3}{x_e y_e^2} & 0 & 0 & \frac{12AB^3}{x_e y_e^3} & 0 & \frac{6AB^3}{x_e y_e^2} & 0 & 0 & -\frac{12AB^3}{x_e y_e^2} & 0 & \frac{6B^3A}{x_e y_e^2} & 0 & 0 & \frac{12AB^3}{x_e y_e^3} & 0 & -\frac{6AB^3}{x_e y_e^2} \end{bmatrix} \quad \text{(A.3)}$$

Displacement vector $\{\delta\}$

$$\{\delta\} = \{U_i, V_i, W_i, W_{i,x}, W_{i,y}, U_j, V_j, W_j, W_{j,x}, W_{j,y}, U_k, V_k, W_k, W_{k,x}, W_{k,y}, U_l, V_l, W_l, W_{l,x}, W_{l,y}\}^T \quad \text{(A.4)}$$

Matrix Q (6 × 20)

$$[Q] = \begin{bmatrix}
0 & \frac{1}{A} & 0 & \frac{y}{AB} & 0 & 0 & 0 & 0 & 0 & 0 & 0 & 0 & 0 & 0 & 0 & 0 & 0 & 0 & 0 & 0 \\
0 & 0 & 0 & 0 & 0 & 0 & \frac{1}{B} & \frac{x}{AB} & 0 & 0 & 0 & 0 & 0 & 0 & 0 & 0 & 0 & 0 & 0 & 0 \\
0 & 0 & \frac{1}{B} & \frac{x}{BA} & 0 & \frac{1}{A} & 0 & \frac{y}{BA} & 0 & 0 & 0 & 0 & 0 & 0 & 0 & 0 & 0 & 0 & 0 & 0 \\
0 & 0 & 0 & 0 & 0 & 0 & 0 & 0 & 0 & 0 & 0 & -\frac{1}{A^2} & 0 & 0 & -\frac{x}{A^3} & -\frac{y}{BA^2} & 0 & 0 & -\frac{xy}{BA^3} & 0 \\
0 & 0 & 0 & 0 & 0 & 0 & 0 & 0 & 0 & 0 & 0 & 0 & 0 & -\frac{1}{B^2} & 0 & 0 & -\frac{x}{B^2A} & -\frac{y}{B^3} & 0 & -\frac{xy}{AB^3} \\
0 & 0 & 0 & 0 & 0 & 0 & 0 & 0 & 0 & 0 & 0 & 0 & -\frac{2}{BA} & 0 & 0 & -\frac{2x}{BA^2} & -\frac{2y}{B^2A} & 0 & -\frac{x^2}{BA^3} & -\frac{y^2}{AB^3}
\end{bmatrix} \quad \text{(A.5)}$$

Matrix P (6 × 6)

In the case of isotropic material the non vanishing terms of the elasticity matrix are

$$P_{11} = P_{22} = D,\ P_{44} = P_{55} = K,\ P_{12} = P_{21} = \nu D,\ P_{45} = P_{54} = \nu K,\ P_{33} = (1-\nu)D/2,\ P_{66} = (1-\nu)K/2 \quad \text{(A.6)}$$

where $K = Eh^3/12(1-\nu^2)$ and $D = Eh/(1-\nu^2)$

Mass and stiffness matrices in local co-ordinates

We rearrange the matrices (mass and stiffness) in order to facilitate the passage to the global coordinates.

$$[k]^e = \begin{bmatrix}
[k_{ii}] & [k_{ij}] & [k_{ik}] & [k_{il}] \\
 & [k_{jj}] & [k_{jk}] & [k_{jl}] \\
 & & [k_{kk}] & [k_{kl}] \\
Sym & & & [k_{ll}]
\end{bmatrix} \quad \text{(A.7)}$$

$$[k']^e = \begin{bmatrix}
[k_{ii}] & \{0\} & [k_{ij}] & \{0\} & [k_{ik}] & \{0\} & [k_{il}] & \{0\} \\
 & 0 & \{0\}^T & 0 & \{0\}^T & 0 & \{0\}^T & 0 \\
 & & [k_{jj}] & \{0\} & [k_{jk}] & \{0\} & [k_{jl}] & \{0\} \\
 & & & 0 & \{0\}^T & 0 & \{0\}^T & 0 \\
 & & & & [k_{kk}] & \{0\} & [k_{kl}] & \{0\} \\
 & & & & & 0 & \{0\}^T & 0 \\
 & & & & & & [k_{ll}] & \{0\} \\
Sym & & & & & & & 0
\end{bmatrix} \quad \text{(A.8)}$$